Mechatronics 23 (2013) 409–418

Contents lists available at SciVerse ScienceDirect

Mechatronics

journal homepage: www.elsevier.com/locate/mechatronics

Sequential co-design of an artifact and its controller via control proxy functions

Diane L. Peters *, Panos Y. Papalambros, A. Galip Ulsoy

Mechanical Engineering Department, University of Michigan, Ann Arbor, MI 48109, USA

ARTICLE INFO

Article history:
Received 2 June 2012
Accepted 7 March 2013
Available online 8 April 2013

Keywords:
Co-design
Design optimization
Controller design
Active suspension
Control proxy function

ABSTRACT

Optimization of a 'smart' product requires optimizing the design of both the physical system, or artifact, and its controller. If the artifact and control optimization are coupled, then a combined approach is typically used in order to produce optimal solutions. The combined approach presents certain disadvantages, however. This combined approach obviates a natural decomposition of the problem into smaller design and control sub-problems that can be a disadvantage from a modeling and solution practicality viewpoint. In this paper, it is shown that a modified sequential approach utilizing a Control Proxy Function (CPF) can be used to produce optimal, or near-optimal, solutions while allowing this decomposition. Two physical bases for CPFs are presented, natural frequency and the controllability Grammian matrix, and their range of applicability is discussed. These concepts are demonstrated, for a positioning gantry example and on an active/passive automotive suspension, to be quite effective.

1. Introduction

The design of many engineered systems requires both the design of the physical system, or artifact, and a controller. In the optimal design and control of such 'smart' systems, it is necessary to specify one or more objectives for the system. In some cases, a single objective function may adequately capture the system's performance. In other cases, there are tradeoffs between different system objectives. If two objectives are present, with one of these objectives primarily identified with the artifact and a second with the controller, then both an artifact objective function, f_a, and a control objective function, f_c, may be formulated, subject to artifact inequality and equality constraints, $\mathbf{g_a}$ and $\mathbf{h_a}$, and control inequality and equality constraints, $\mathbf{g_c}$ and $\mathbf{h_c}$. These objectives and constraints are functions of artifact and controller design variables, denoted as $\mathbf{d_a}$ and $\mathbf{d_c}$, respectively. In the most general case, all of the objectives and constraints may be functions of both sets of variables, i.e., $F_a = f_a(\mathbf{d_a},\mathbf{d_c})$, $\mathbf{G_a} = \mathbf{g_a}(\mathbf{d_a},\mathbf{d_c})$, $\mathbf{H_a} = \mathbf{h_a}(\mathbf{d_a},\mathbf{d_c})$, $F_c = f_c(\mathbf{d_a},\mathbf{d_c})$, $\mathbf{G_c} = \mathbf{g_c}(\mathbf{d_a},\mathbf{d_c})$, and $\mathbf{H_c} = \mathbf{h_c}(\mathbf{d_a},\mathbf{d_c})$. This optimal design and control problem, denoted as co-design, can present special challenges when the design of the artifact and controller are dependent on one another. In this situation, the solution of the bi-objective co-design problem given by Eq. (1) is a Pareto set, with the various Pareto points found by varying the weights w_a and w_c, and the problem is said to be coupled.

$$\begin{aligned} \min_{\mathbf{d_a},\mathbf{d_c}} \quad & w_a f_a(\mathbf{d_a},\mathbf{d_c}) + w_c f_c(\mathbf{d_a},\mathbf{d_c})(\mathbf{d_a},\mathbf{d_c}) \\ \text{subject to} \quad & \mathbf{g_a} \leqslant \mathbf{0} \\ & \mathbf{h_a}(\mathbf{d_a},\mathbf{d_c}) = \mathbf{0} \\ & \mathbf{g_c}(\mathbf{d_a},\mathbf{d_c}) \leqslant \mathbf{0} \\ & \mathbf{h_c}(\mathbf{d_a},\mathbf{d_c}) = \mathbf{0} \end{aligned} \tag{1}$$

When all of the objective and constraint functions depend on both $\mathbf{d_a}$ and $\mathbf{d_c}$, coupling is said to be bi-directional. Many such problems exist, such as the design of mechanisms subject to constraints on stress or deflection as they are moving. However, there is also a large class of problems in which neither the artifact objective function nor the artifact constraints are functions of $\mathbf{d_c}$, i.e., $F_a = f_a(\mathbf{d_a})$, $\mathbf{G_a} = \mathbf{g_a}(\mathbf{d_a})$, and $\mathbf{H_a} = \mathbf{h_a}(\mathbf{d_a})$. These problems are said to exhibit uni-directional coupling. The method presented in this paper is developed for problems that exhibit uni-directional coupling. It is also shown, through one of the examples, that it can be applied to some problems with bi-directional coupling.

A variety of measures have been proposed to quantify the strength of coupling [1–6]. These measures have been shown to be related, though in most cases they are not commensurate with one another [7–9]. In problems with uni-directional coupling, one measure which is particularly useful is the coupling vector, $\mathbf{\Gamma_v}$, which is defined as follows [3,10].

$$\mathbf{\Gamma_v} = \frac{w_c}{w_a}\left(\frac{\partial f_c(\mathbf{d_a},\mathbf{d_c})}{\partial \mathbf{d_a}} + \frac{\partial f_c(\mathbf{d_a},\mathbf{d_c})}{\partial \mathbf{d_c}}\frac{d\mathbf{d_c}}{d\mathbf{d_a}}\right) \tag{2}$$

This vector is valid only at an optimal solution; however, at a point not known to be optimal, an estimate can be computed. The equation for the estimated coupling vector, denoted

* Corresponding author. Tel.: +1 248 502 2330; fax: +1 248 952 1610.
E-mail addresses: dlpeters@umich.edu (D.L. Peters), pyp@umich.edu (P.Y. Papalambros), ulsoy@umich.edu (A.G. Ulsoy).

0957-4158/$ - see front matter © 2013 Elsevier Ltd. All rights reserved.
http://dx.doi.org/10.1016/j.mechatronics.2013.03.003

as $\widehat{\mathbf{\Gamma}}_{\mathbf{v}}$, is identical to Eq. (2), but does not require the solution of Eq. (1).

Coupled systems reported in the literature are in diverse areas including structural systems with active control (e.g., [1,11]), micro-electrical mechanical systems, or MEMS (e.g., [12,13]), automotive systems (e.g., [10,14,15]), robotics and mechatronics (e.g., [16–20]), and various types of mechanisms and machine tools (e.g., [21–24]). In robotic applications, typical objectives for the artifact design are minimizing weight or minimizing deflection. Controller objectives may be minimizing tracking errors for a particular trajectory, overshoot, or settling time [25]. In these problems, speed and accuracy are in conflict; mechanisms with lower inertia are more flexible, resulting in a fast response but lower accuracy, while a higher inertia will produce a stiffer mechanism that is more accurate but results in lower speeds [19]. Many applications, however, require both high speed and high accuracy. Therefore, design of such systems must consider the coupling between the artifact and control objectives [26].

It has been shown that a simple sequential optimization, in which the artifact is first optimized and then the optimal control is found for that artifact, does not find the optimum for the system [27,28]. Combined optimization methods such as a simultaneous strategy, in which both the artifact and control are optimized together, will produce system-optimal solutions, as demonstrated in [27,28]. The larger combined problem increases computational complexity, and may require closer coordination of modeling efforts from different groups in the organization. Furthermore, while some methods such as pseudo-spectral methods [29] can be used for a combined problem, classical optimal control techniques can no longer be used when the problem is not formulated as a purely optimal control problem [8].

Previous work has shown that the use of a Control Proxy Function (CPF) can provide optimal, or near-optimal, solutions to the co-design problem without the disadvantages seen in the combined optimization techniques, and has set forth the mathematical conditions under which such a CPF is effective [8,9]. In this paper, the work described in [30] is expanded, both theoretically and in the examples shown. It is shown that, in addition to the cases described in [30], it is possible to formulate a CPF based on the controllability Grammian matrix for some LQR problems, based on the theoretical developments presented in [9]. It is also shown, through the development of an automotive suspension example, that while the method was developed under the assumption of uni-directional coupling, it may also be used in some cases where bi-directional coupling is present.

2. Optimization of coupled systems using a Control Proxy Function (CPF)

In order to preserve the functional decomposition of the co-design problem while realizing optimal or near-optimal solutions, a modified sequential optimization strategy is proposed. In this strategy, the original artifact objective function, f_a, is augmented with a Control Proxy Function (CPF), representing the system's ease of control, as shown in Fig. 1. The CPF, denoted as χ, is a function only of the artifact design variables, $\mathbf{d_a}$. The optimization problem is then formulated as follows:

$$\begin{aligned} \min_{\mathbf{d_a}} \quad & f'_a(\mathbf{d_a}) = w_1 f_a(\mathbf{d_a}) + w_2 \chi(\mathbf{d_a}) \\ \text{subject to} \quad & \mathbf{g_a}(\mathbf{d_a}) \leqslant \mathbf{0} \\ & \mathbf{h_a}(\mathbf{d_a}) = \mathbf{0} \end{aligned} \tag{3}$$

where w_1 and w_2 are positive weights representing the relative importance of the artifact objective and the CPF, followed by the control design problem

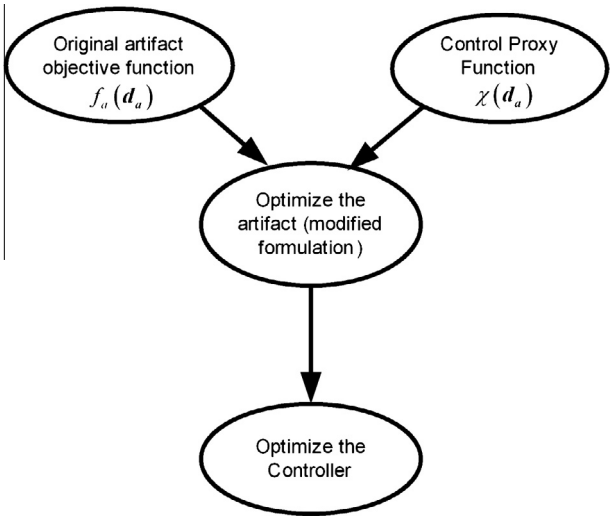

Fig. 1. Control proxy function problem formulation.

$$\begin{aligned} \min_{\mathbf{d_c}} \quad & f_c(\mathbf{d}^*_{\mathbf{a}}, \mathbf{d_c}) \\ \text{subject to} \quad & \mathbf{g_c}(\mathbf{d}^*_{\mathbf{a}}, \mathbf{d_c}) \leqslant \mathbf{0} \\ & \mathbf{h_c}(\mathbf{d}^*_{\mathbf{a}}, \mathbf{d_c}) = \mathbf{0} \end{aligned} \tag{4}$$

where $\mathbf{d}^*_{\mathbf{a}} = \text{argmin} f'_a(\mathbf{d_a})$.

The success of the method depends on the selection of an appropriate CPF. A well-chosen CPF, which effectively captures the fundamental physical limitations of the system, will result in solutions that are close to the Pareto optimal points found by a simultaneous formulation, while a poorly chosen CPF will yield solutions far from system optimality.

The theoretical properties of an effective CPF have been studied, and four theorems describing appropriate CPFs have been proven [8,9]. These theorems are summarized here as follows:

1. If $\mathbf{\Gamma_v}$ is parallel to $\nabla\chi$ at all points, then the CPF solution set will coincide with the Pareto frontier. A CPF satisfying this condition is said to be perfect.
2. CPF solution points will approach the Pareto frontier as ξ, the angle between the estimate of the coupling vector $\widehat{\mathbf{\Gamma}}_{\mathbf{v}}$ and $\nabla\chi$ in the $\mathbf{d_a}$-space, approaches zero; i.e., CPF solution points will be close to the Pareto frontier when the angle ξ is small.
3. If the control objective function, $f_c(\mathbf{d_a}, \mathbf{d_c})$, is monotonic with respect to some element of $\mathbf{d_a}$, then an effective CPF, $\chi(\mathbf{d_a})$, will have the same coordinate-wise monotonicity as f_c with respect to that element of $\mathbf{d_a}$.
4. If the control objective function, $f_c(\mathbf{d_a}, \mathbf{d_c})$, has an unconstrained minimum in the $\mathbf{d_a}$-space, then an effective CPF, $\chi(\mathbf{d_a})$, will obtain its minimum close to it.

In this paper, Theorem (1) will be particularly useful, as it can be used to determine under what conditions the particular CPFs considered will produce optimal solutions. Theorem (2) will be used to evaluate the solutions found when the CPF method is applied to an example problem.

Having developed a theoretical basis for an effective CPF in [8,9], a logical next step is to formulate specific CPFs for important types of problems and evaluate them. Initial work in this area was shown in [30] and expanded here. These specific CPFs are based on physically meaningful system characteristics, specifically the natural frequency of the system and the controllability Grammian matrix. The natural frequency is considered as the basis for a CPF

because previous work has shown that, in some cases, it can be used as an effective proxy for a system's ease of control (e.g., [30–33]). The use of natural frequency as a CPF is considered in Section 3, along with an application to a simple positioning gantry. The controllability Grammian matrix, $\mathbf{W_c}$, will be considered as the basis for a CPF because it has been successfully used for the location of actuators (e.g., [34–36]). Furthermore, it has been shown that, for some problem formulations, there is a relationship between $\mathbf{W_c}$ and the coupling vector $\mathbf{\Gamma_v}$ [37]. Since there is also a relationship between $\mathbf{\Gamma_v}$ and an effective CPF, as outlined above, this suggests that a CPF based on $\mathbf{W_c}$ will be perfect for some problems, and this is shown in [30]. In Section 4, the use of a CPF based on the controllability Grammian is presented, and applied to the design of a passive/active automotive suspension. These two types of CPFs are neither exhaustive normutually exclusive; there could be problems where the conditions are met for both a CPF based on natural frequency and for a CPF based on the controllability Grammian matrix. If this were the case, then either physical basis could be chosen, based on the preference of the designer.

3. Control proxy function utilizing natural frequency

3.1. Problem formulation

The natural frequency has been successfully used to predispose a system to effective control, suggesting that it can be used to formulate an effective control proxy function in some cases. Naturally, the question arises what those cases might be, and how they can be identified. Here, three specific problem formulations are presented, derived in [8,30], in which natural frequency can be used in a perfect CPF. Those system characteristics that are common to all three problems are:

1. The co-design problem is formulated as in Eq. (1), and exhibits uni-directional coupling.
2. The system is linear and dominated by second-order dynamics. This system can be described, then, in the form

$$m\ddot{z} + b\dot{z} + kz = u(t) \tag{5}$$

where m, b, and k are functions of the design variables d_a, parameters, and constants, z is the system output, and $u(t)$ is the forcing function; or alternatively in state-space form as

$$\dot{\mathbf{x}} = \mathbf{A}\mathbf{x} + \mathbf{B}u \tag{6}$$

where

$$\mathbf{A} = \begin{bmatrix} 0 & 1 \\ -\frac{k}{m} & -\frac{b}{m} \end{bmatrix} \tag{7}$$

$$\mathbf{B} = \begin{bmatrix} 0 \\ \frac{1}{m} \end{bmatrix} \tag{8}$$

$$\mathbf{x} = \begin{bmatrix} z \\ \dot{z} \end{bmatrix} \tag{9}$$

The open-loop system is underdamped, i.e., the open-loop eigenvalues are complex.

3. The matrix $\mathbf{B}$ is independent of the artifact design variables $\mathbf{d_a}$, i.e.,

$$\frac{\partial m}{\partial \mathbf{d_a}} = \mathbf{0}. \tag{10}$$

4. A state-feedback controller with gains $\mathbf{K} = [K_1\ K_2]$, possibly with a precompensator G, is applied to the system, as shown in Fig. 2.

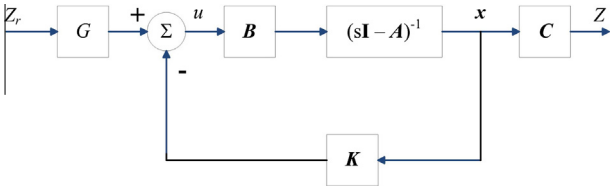

Fig. 2. Schematic of system controller.

5. There are no active controller equality constraints $\mathbf{h_c}(\mathbf{d_a}, \mathbf{d_c})$ or strongly active controller inequality constraints $\mathbf{g_c}(\mathbf{d_a}, \mathbf{d_c})$ present. Weakly active controller inequality constraints may be present, where a weakly active constraint is one which is not satisfied as a strict equality but whose removal will affect the system optimum [38].

In a second-order system, there are two eigenvalues, which are complex conjugates. These eigenvalues can be fully described by the frequency ω and damping coefficient ζ of the system.

$$\lambda_{1,2} = -\zeta\omega \pm \omega\sqrt{\zeta^2 - 1} \tag{11}$$

The natural frequency of the open-loop system will be denoted as ω_n and the damping coefficient of the open-loop system as ζ_n. The frequency of the controlled, or closed-loop, system will be denoted as ω_c and the damping coefficient of the closed-loop system will be denoted as ζ_c. The open-loop and closed-loop frequencies and damping coefficients for the second-order system subjected to state-feedback control are given by the following equations [39]:

$$\omega_n = \sqrt{\frac{k}{m}} \tag{12}$$

$$\zeta_n = \frac{b}{2\sqrt{mk}} \tag{13}$$

$$\omega_c = \sqrt{\frac{k + K_1}{m}} \tag{14}$$

$$\zeta_c = \frac{b + K_2}{2\sqrt{m(k + K_1)}} \tag{15}$$

These equations will be used to define three specific problem formulations where $\chi(\mathbf{d_a}) = \chi(\omega_n)$ is a perfect CPF. In each case, additional necessary conditions are specified, relating to the damping of the system.

3.1.1. Control objective independent of damping

If the control objective $F_c = f_c(\omega_c)$ is a function of the closed-loop frequency ω_c of the system but is independent of the closed-loop damping coefficient ζ_c, then the CPF $\chi = \chi(\omega_n)$ will yield system-optimal solutions to the simultaneous optimization problem. An example of such a control objective is $f_c(\omega_c) = t_r$, where $t_r = \frac{1.8}{\omega_c}$ is the rise time of the closed-loop system [39]. For a second-order system, ω_n is given by Eq. (12), and therefore the gradient of χ is given by

$$\nabla\chi = \frac{\partial\chi}{\partial\omega_n}\frac{\partial\omega_n}{\partial\mathbf{d_a}} = \frac{\partial\chi}{\partial\omega_n}\left(\frac{1}{2}\sqrt{\frac{1}{km}}\frac{\partial k}{\partial\mathbf{d_a}}\right) \tag{16}$$

where k is a function of $\mathbf{d_a}$. The closed-loop frequency of the system is given by Eq. (14). Using Eq. (2), the coupling is found to be

$$\mathbf{\Gamma_v} = \frac{w_2}{w_1}\frac{\partial f_c(\omega_c)}{\partial\omega_c}\left(\frac{1}{2}\sqrt{\frac{1}{(k + K_1)m}}\frac{\partial k}{\partial\mathbf{d_a}}\right) \tag{17}$$

If the CPF is perfect, the vector computed is the coupling vector $\mathbf{\Gamma_v}$, not the estimate $\widehat{\mathbf{\Gamma}}_\mathbf{v}$. It is possible, then, to express the coupling vector $\mathbf{\Gamma_v}$ at the CPF solution as

$$\mathbf{\Gamma_v} = \frac{w_2}{w_1}\sqrt{\frac{k}{k+K_1}}\left(\left(\frac{\partial f_c(\omega_c)}{\partial \omega_c}\right)\Big/\left(\frac{\partial \chi}{\partial \omega_n}\right)\right)\nabla\chi \tag{18}$$

and it can be seen that the coupling vector at the CPF point is equal to a scalar quantity multiplied by the gradient of the CPF. From Theorem 1, then, the CPF points will be Pareto optimal for the co-design problem.

3.1.2. Control objective independent of imaginary component of eigenvalues

If the control objective $F_c = f_c(\zeta_c\omega_c)$ is a function of the real part of the closed-loop eigenvalues (e.g., $f_c(\zeta_c\omega_c) = t_s$, where t_s is the settling time of the closed-loop system), and the damping ratio ζ_n of the open-loop system is independent of $\mathbf{d_a}$, then the CPF $\chi = \chi(\omega_n)$ will yield system-optimal solutions to the simultaneous optimization problem.

A similar procedure to that given above [8] can be used to derive a relationship between the coupling vector and the gradient $\nabla\chi$. This relationship is found to be

$$\mathbf{\Gamma_v} = \frac{w_2}{w_1}\frac{\partial f_c(\zeta_c\omega_c)}{\partial(\omega_c\zeta_c)}\frac{b}{2\sqrt{km}}\left(1\Big/\frac{\partial\chi}{\partial\omega_n}\right)\nabla\chi \tag{19}$$

Again, if the CPF is perfect, the vector computed is the coupling vector $\mathbf{\Gamma_v}$, not the estimate $\widehat{\mathbf{\Gamma}}_\mathbf{v}$. It can then be seen that the coupling vector at the CPF point is equal to a scalar multiplied by $\nabla\chi$, where $\nabla\chi$ is given by Eq. (16). Therefore, from Theorem 1, the CPF points will be Pareto optimal for the co-design problem.

3.1.3. Damping term b independent of d_a

If the controller objective $F_c = f_c(\zeta_c, \omega_c)$ is an arbitrary function of the closed-loop eigenvalues of the system, and the damping term b in the system description is independent of $\mathbf{d_a}$, i.e.,

$$\frac{\partial b}{\partial \mathbf{d_a}} = \mathbf{0} \tag{20}$$

then the CPF $\chi = \chi(\omega_n)$ will yield system-optimal solutions to the simultaneous optimization problem.

Yet again, as shown in [8], a relationship can be derived between the coupling vector and the gradient $\nabla\chi$. This relationship is found to be

$$\mathbf{\Gamma_v} = \frac{w_2}{w_1}\sqrt{\frac{k}{k+K_1}}\left(\frac{\partial f_c(\zeta_c,\omega_c)}{\partial\omega_c} - \frac{\partial f_c(\zeta_c,\omega_c)}{\partial\zeta_c}\frac{b+K_2}{2(k+K_1)}\right)\left(1/\frac{\partial\chi}{\partial\omega_n}\right)\nabla\chi \tag{21}$$

Again, if the CPF is perfect, the vector computed is the coupling vector $\mathbf{\Gamma_v}$, not the estimate $\widehat{\mathbf{\Gamma}}_\mathbf{v}$. It can be seen that the coupling vector at the CPF point is equal to a scalar multiplied by $\nabla\chi$, where $\nabla\chi$ is given by Eq. (16). Therefore, from Theorem 1, the CPF points will be Pareto optimal for the co-design problem.

3.2. Illustrative example: positioning gantry system

Consider the system shown in Fig. 3, representing a simple model of a positioning gantry. In this system, a mass M is connected to a fixed surface by a linear spring with constant k_s. A flexible belt connects to the mass and wraps around a pulley with radius r, which is mounted on a DC motor with armature resistance R_a and motor constant k_t. The displacement of the mass from its original position is Z. The system can be modeled in the form of Eqs. (5)–(9), where $m = \frac{MrR_a}{k_t}$, $b = \frac{k_t}{r}$, and $k = \frac{k_s r R_a}{k_t}$. A state-feedback controller with gains $\mathbf{K} = [K_1\ K_2]$ and precompensator G is applied

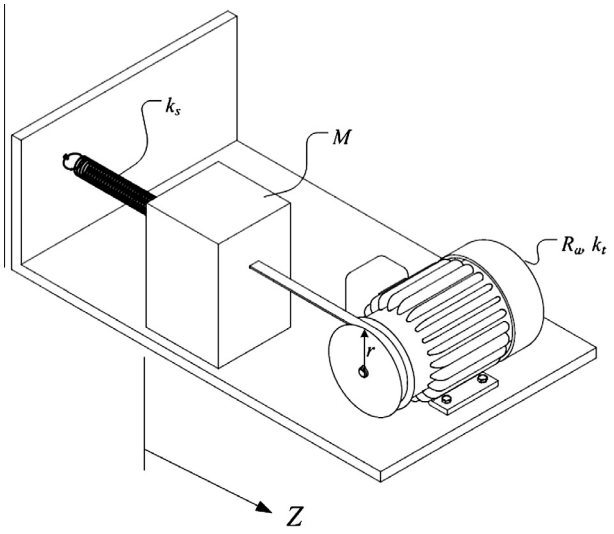

Fig. 3. Configuration of positioning gantry system.

to the system, as shown in Fig. 2, to generate the input voltage u to the motor. The steady-state voltage is denoted as u_{ss}. Values of parameters are given as $k_t = 10.0$ N m/A, $r = 5.0$ cm, $M = 2.0$ kg, and $u_{ss} = 10.0$ V.

The following objectives and constraints are selected:

$$f_a(R_a, k_s) = -Z_{ss} \tag{22}$$

subject to simple bounds on the artifact design variables:

$$2.0\ \text{k}\Omega \leqslant R_a \leqslant 3.0\ \text{k}\Omega \tag{23}$$

$$0.5\ \text{N/mm} \leqslant k_s \leqslant 5.5\ \text{N/mm} \tag{24}$$

where Z_{ss} is the steady-state displacement, given by

$$Z_{ss} = \frac{u_{ss}k_t}{rR_ak_s} \tag{25}$$

The controller objective is the 1% settling time for the system, t_s, which is given by

$$f_c(R_a, k_s, K_1, K_2, G) = \frac{4.6MR_ar}{k_t(rK_2 + k_t)} \tag{26}$$

with constraints on the overshoot, M_p, and the peak motor voltage, u_p, as given below.

$$M_p \leqslant 5\% \tag{27}$$

$$u_p \leqslant 12.5\ \text{V} \tag{28}$$

The optimization problem is formulated as in Eqs. (3) and (4), using the natural frequency of the open-loop system as the CPF. Since the damping term b is not a function of the artifact design variables, it is expected that the solutions found will be system-optimal, as shown in Section 3.1.

This problem was solved using Matlab's *fmincon* function for a variety of weights w_1 and w_2, producing the results for the Pareto curve shown in Fig. 4. For each point, $\nabla\chi$ and $\widehat{\mathbf{\Gamma}}_\mathbf{v}$ were calculated. Using these vectors, the angle ξ was calculated, and it was found that $\xi = 0$ for all points. Thus, based on Theorem (2), it is known that these solutions are system-optimal. Note that this was determined without the need to solve the simultaneous problem in Eq. (1). While there are only small computational gains in this case, the primary advantage of this solution method for this problem is that it allows the design and control optimizations to be carried out separately. The designer of the gantry system then would not need to also design the control system, and that task could be left to a

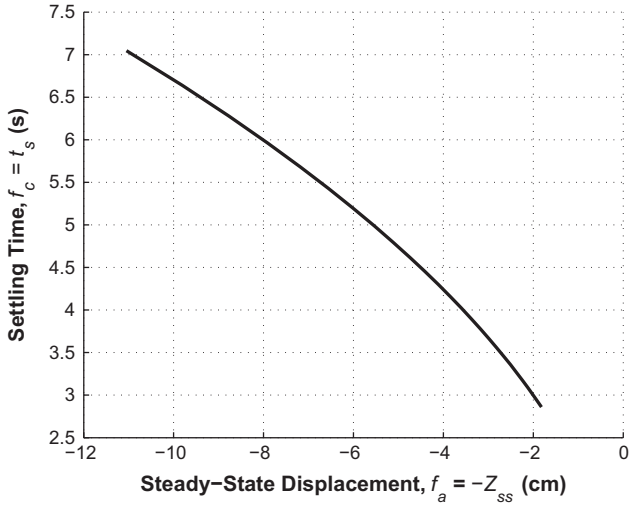

Fig. 4. Results of positioning gantry optimization.

specialist in controls while ensuring the system optimal design for the gantry and its controller.

4. Control proxy function utilizing the controllability Grammian matrix

4.1. Problem formulation

A CPF using open-loop eigenvalues will not be effective when the matrix **B** in Eq. (6) is sensitive to the artifact design variables $\mathbf{d_a}$, since open-loop eigenvalues cannot be used to model that system behavior. For problems of this type, the CPF must be based on some other fundamental metric of the system which is capable of modeling both the free and forced response characteristics of the system. Since the controllability Grammian matrix $\mathbf{W_c}$ incorporates both the free and forced response characteristics of a system, it is logical to consider its use in a CPF. Here, we will demonstrate that the controllability Grammian can be used to formulate a CPF in some cases. Additional cases in which the controllability Grammian can be used are given in [8].

In the development of the CPF based on the controllability Grammian, it is assumed that the system dynamics are linear and time-invariant, and can be described in state-space form, i.e., by Eq. (6). The system may be of arbitrarily high order, rather than second-order as in the previous section. For this system, the time-varying controllability Grammian matrix is given by [40]

$$\mathbf{W_c}(t_f) = \int_0^{t_f} e^{\mathbf{A}t}\mathbf{B}\mathbf{B}^T e^{\mathbf{A}^T t}dt \tag{29}$$

and the steady-state controllability Grammian matrix is given by

$$\mathbf{W_c^\infty} = \lim_{t_f\to\infty}\int_0^{t_f} e^{\mathbf{A}t}\mathbf{B}\mathbf{B}^T e^{\mathbf{A}^T t}dt \tag{30}$$

The CPF that will be first considered is:

$$\chi = \mathbf{x_f^T}\mathbf{W_c^{-1}}(t_f)\mathbf{x_f} \tag{31}$$

where $\mathbf{x_f}$ is the final state of the system, and t_f is the time at which it reaches that state.

4.1.1. Control effort as control objective function

The CPF given by Eq. (31) will produce optimal solutions when the control objective function, f_c, is the control effort necessary to move the system from its zero state to its final state, $\mathbf{x_f}$, at a specified final time, t_f, where t_f is a parameter. The final state, $\mathbf{x_f}$, may be a parameter or it can be a function of the artifact design variables, $\mathbf{d_a}$. An example would be a positioning device in an automated assembly system; parts to be assembled typically must be placed at their destination at a particular time.

The objective function, f_c, is given by

$$f_c = \int_0^{t_f} (u(t))^2 dt. \tag{32}$$

The controllability Grammian matrix can be used to construct a lower bounding function for the control effort, which is given by [40]

$$f_c \geqslant \mathbf{x_f^T}\mathbf{W_c^{-1}}(t_f)\mathbf{x_f} \tag{33}$$

If an optimal controller is used, then the optimal value of f_c is given by

$$f_c^* = \mathbf{x_f^T}\mathbf{W_c^{-1}}(t_f)\mathbf{x_f}, \tag{34}$$

and it is evident that the solutions found using this CPF will be optimal since $\chi = f_c$. Furthermore, it has been shown that [37], for this problem,

$$\mathbf{\Gamma_v} = \frac{w_c}{w_a}\frac{\partial}{\partial \mathbf{d_a}}\left(\mathbf{x_f^T}\mathbf{W_c^{-1}}(t_f)\mathbf{x_f}\right), \tag{35}$$

and thus Theorem (1) confirms that the CPF given in Eq. (31) will produce optimal solutions.

4.1.2. Time as control objective function and control effort as constraint

The CPF given by Eq. (31) will produce optimal solutions when the control objective function is the time, t_f, necessary to move the system from its zero state to a final state, $\mathbf{x_f}$, subject to a limit on the available control energy, E_{max}, where E_{max} is a parameter. Again, $\mathbf{x_f}$ may be a parameter or a function of $\mathbf{d_a}$.

The objective function, f_c, and constraint, g_c, are given by

$$f_c = t_f \tag{36}$$

$$g_c = \int_0^{t_f} (u(t))^2 dt - E_{max} \leqslant 0 \tag{37}$$

The coupling vector for this problem is parallel to that for the problem where control effort is the objective function. Therefore, the coupling vector for this problem will also be parallel to $\nabla\chi$, where χ is given by Eq. (31). Using Theorem (1), it can be seen that the use of this CPF will result in optimal solutions.

4.1.3. Control proxy function for the case of Linear Quadratic Regulator (LQR)

The infinite-time LQR problem is designed to find the optimal control signal $\mathbf{u}(t)$ to transition a system from an initial state $\mathbf{x_0} = \mathbf{x}(0)$ to the zero state. The optimal control signal is defined as the one which minimizes the cost function

$$J = \int_0^\infty (\mathbf{x}(t)^T\mathbf{Q}\mathbf{x}(t) + \mathbf{u}(t)^T\mathbf{R}\mathbf{u}(t))dt. \tag{38}$$

It is well-established [40] that the optimal solution is

$$\mathbf{u}(t) = -\mathbf{K}\mathbf{x}(t) \tag{39}$$

$$\mathbf{K} = \mathbf{R}^{-1}\mathbf{B}^T\mathbf{X} \tag{40}$$

where the matrix **X** is the positive semi-definite solution of the algebraic Riccati equation

$$\mathbf{A}^T\mathbf{X} + \mathbf{X}\mathbf{A} - \mathbf{X}\mathbf{B}\mathbf{R}^{-1}\mathbf{B}^T\mathbf{X} + \mathbf{Q} = 0 \tag{41}$$

and the optimal value of J is given by the equation

$$J^* = \mathbf{x_0^T}\mathbf{X}\mathbf{x_0}. \tag{42}$$

As shown in [8,37], the coupling vector for the LQR problem can be related to the controllability Grammian for the specific choice of the state weighting matrix $\mathbf{Q} = \gamma \mathbf{B}\mathbf{B}^T$, which is commonly used in loop-transfer recovery. For this particular choice of $\mathbf{Q}$, it can be shown that the matrix $\mathbf{X}$ can be expressed in terms of the controllability Grammian as [8,37]:

$$\mathbf{X} = \gamma \mathbf{A}^{-T} \mathbf{A} \mathbf{W}_{\mathbf{c}}^{\infty} \tag{43}$$

and, therefore, the optimal performance is

$$J^* = \gamma \mathbf{x}_0^T \mathbf{A}^{-T} \mathbf{A} \mathbf{W}_{\mathbf{c}}^{\infty} \mathbf{x}_0. \tag{44}$$

This allows the coupling to be derived as

$$\mathbf{\Gamma}_{\mathbf{v}} = \gamma \frac{w_c}{w_a} \begin{bmatrix} \frac{\partial \left(\mathbf{x}_0^T \mathbf{A}^{-T} \mathbf{A} \mathbf{W}_{\mathbf{c}}^{\infty} \mathbf{x}_0 \right)}{\partial d_{a_1}} \\ \frac{\partial \left(\mathbf{x}_0^T \mathbf{A}^{-T} \mathbf{A} \mathbf{W}_{\mathbf{c}}^{\infty} \mathbf{x}_0 \right)}{\partial d_{a_2}} \\ \vdots \\ \frac{\partial \left(\mathbf{x}_0^T \mathbf{A}^{-T} \mathbf{A} \mathbf{W}_{\mathbf{c}}^{\infty} \mathbf{x}_0 \right)}{\partial d_{a_n}} \end{bmatrix}^T \tag{45}$$

In the most general LQR case, the initial state $\mathbf{x_0}$, $\mathbf{W}_{\mathbf{c}}^{\infty}$, and $\mathbf{A}$ all depend on $\mathbf{d_a}$. For this case, a perfect CPF will be one with a gradient parallel to the coupling vector. If a CPF is chosen to be

$$\chi(\mathbf{d_a}) = \mathbf{x}_0^T \mathbf{A}^{-T} \mathbf{A} \mathbf{W}_{\mathbf{c}}^{\infty} \mathbf{x_0} \tag{46}$$

then the gradient of this CPF is given by

$$\frac{\partial \chi}{\partial \mathbf{d_a}} = \frac{\partial}{\partial \mathbf{d_a}} \left(bmx_0^T \mathbf{A}^{-T} \mathbf{A} \mathbf{W}_{\mathbf{c}}^{\infty} \mathbf{x_0} \right) = \begin{bmatrix} \frac{\partial \left(\mathbf{x}_0^T \mathbf{A}^{-T} \mathbf{A} \mathbf{W}_{\mathbf{c}}^{\infty} \mathbf{x}_0 \right)}{\partial d_{a_1}} \\ \frac{\partial \left(\mathbf{x}_0^T \mathbf{A}^{-T} \mathbf{A} \mathbf{W}_{\mathbf{c}}^{\infty} \mathbf{x}_0 \right)}{\partial d_{a_2}} \\ \vdots \\ \frac{\partial \left(\mathbf{x}_0^T \mathbf{A}^{-T} \mathbf{A} \mathbf{W}_{\mathbf{c}}^{\infty} \mathbf{x}_0 \right)}{\partial d_{a_n}} \end{bmatrix}^T \tag{47}$$

and it can be shown that

$$\frac{\partial \chi}{\partial \mathbf{d_a}} = \frac{w_c}{w_a} \mathbf{\Gamma}_v \tag{48}$$

and therefore the CPF is perfect for this problem.

4.2. Illustrative example: passive/active automotive suspension

Consider the automotive suspension for a quarter-car model shown in Fig. 5. This suspension is modeled in state-space form with both a control input, u, and an external disturbance, w, by the following equation:

$$\dot{\mathbf{x}}(t) = \mathbf{A}\mathbf{x}(t) + \mathbf{B}u(t) + \mathbf{G}w(t) \tag{49}$$

where

$$\mathbf{A} = \begin{bmatrix} 0 & 1 & 0 & 0 \\ -\frac{k_{us}}{m_{us}} & -\frac{c_s}{m_{us}} & \frac{k_s}{m_{us}} & \frac{c_s}{m_{us}} \\ 0 & -1 & 0 & 1 \\ 0 & \frac{c_s}{m_s} & -\frac{k_s}{m_s} & -\frac{c_s}{m_s} \end{bmatrix} \tag{50}$$

$$\mathbf{B} = \begin{bmatrix} 0, & \frac{1}{m_{us}}, & 0, & -\frac{1}{m_s} \end{bmatrix}^T \tag{51}$$

$$\mathbf{G} = [-1, \quad 0, \quad 0, \quad 0]^T, \tag{52}$$

the set of states, $\mathbf{x}(t)$, is given by

$$\mathbf{x}(t) = [z_{us}(t) - z_g(t), \dot{z}_{us}(t), z_s(t) - z_{us}(t), \dot{z}_s(t)]^T \tag{53}$$

and the ground velocity disturbance $w(t)$ is characterized as zero-mean white noise with a Gaussian distribution, i.e., $E\{\dot{z}_g(t)\dot{z}_g(\tau)\} = W\delta(t-\tau)$ [41].

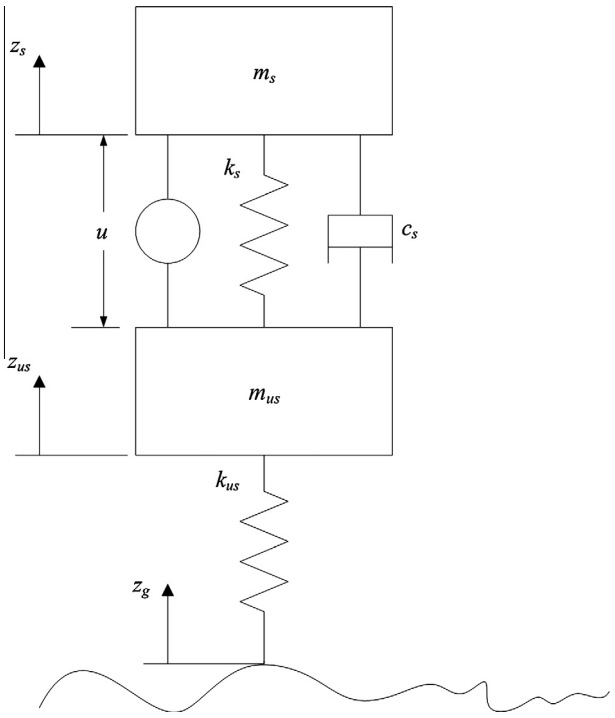

Fig. 5. Quarter-car model of combined active and passive suspension.

The objective functions for the optimization of this system will be the control effort, J_u, and the ride quality, J_q, for the suspension design. As discussed in [41], the ride quality includes the mean square sprung mass acceleration, mean square tire deflection (wheel hop), and mean square suspension stroke (rattle space). These objective functions, and the total system objective, J, are given in Eqs. (54)–(56), where r_0, r_1, r_2, and r_3 are weighting factors selected by the designer of the suspension system based on the desired characteristics of the suspension, e.g., a 'sporty' suspension versus a luxury vehicle's suspension. While the weighting factor r_3 will be varied to produce multiple designs, r_0, r_1, and r_2 will be set as parameters. These, and other parameters, are given in Table 1.

$$J_q = E\left\{ \lim_{T\to\infty} \frac{1}{T} \int_0^T (r_0(\ddot{z}_s)^2 + r_1(z_{us} - z_g)^2 + r_2(z_s - z_{us})^2) dt \right\} \tag{54}$$

$$J_u = E\left\{ \lim_{T\to\infty} \frac{1}{T} \int_0^T u^2 dt \right\} \tag{55}$$

$$J = J_q + r_3 J_u \tag{56}$$

The ride quality can be expressed in terms of the state variables as

$$J_q = E\left\{ \lim_{T\to\infty} \frac{1}{T} \int_0^T (r_0(\dot{x}_4)^2 + r_1(x_1)^2 + r_2(x_3)^2) dt \right\} \tag{57}$$

By substituting for $\dot{x}_4$ from Eqs. (49)–(52), and expanding terms, the total system objective, J, can be written in standard LQR form as

$$J = E\left\{ \lim_{T\to\infty} \frac{1}{T} \int_0^T (\mathbf{x}^T \mathbf{Q}\mathbf{x} + 2\mathbf{x}^T \mathbf{S}\mathbf{u} + \mathbf{u}^T \mathbf{R}\mathbf{u}) dt \right\} \tag{58}$$

Table 1
Automotive suspension parameters.

r_0	r_1	r_2	m_s (kg)	m_{us} (kg)	k_{us} (kN/m)
8.29e−4	414.7	41.47	2000	184	520

where the weighting matrix, $\mathbf{Q}$, is given by

$$\mathbf{Q} = \begin{bmatrix} r_1 & 0 & 0 & 0 \\ 0 & r_0\left(\frac{c_s}{m_s}\right)^2 & -r_0\frac{c_s k_s}{m_s^2} & -r_0\left(\frac{c_s}{m_s}\right)^2 \\ 0 & -r_0\frac{c_s k_s}{m_s^2} & r_2 + r_0\left(\frac{k_s}{m_s}\right)^2 & r_0\frac{c_s k_s}{m_s^2} \\ 0 & -r_0\left(\frac{c_s}{m_s}\right)^2 & r_0\frac{c_s k_s}{m_s^2} & r_0\left(\frac{c_s}{m_s}\right)^2 \end{bmatrix} \tag{59}$$

and the matrices $\mathbf{R}$ and $\mathbf{S}$ are given by

$$\mathbf{R} = \left[r_3 + \frac{r_0}{m_s^2}\right] \tag{60}$$

$$\mathbf{S} = \left[0, \quad -\frac{r_0 c_s}{m_s^2}, \quad \frac{r_0 k_s}{m_s^2}, \quad \frac{r_0 c_s}{m_s^2}\right]^T \tag{61}$$

For a given passive suspension design, it is then possible to find the optimal active suspension. The optimal gains for such a suspension are given by [42,43]

$$\mathbf{K} = \mathbf{R}^{-1}(\mathbf{S}^T + \mathbf{B}^T\mathbf{X}) \tag{62}$$

where the matrix $\mathbf{X}$ is the positive semi-definite solution to the Riccati equation

$$(\mathbf{A} - \mathbf{B}\mathbf{R}^{-1}\mathbf{S}^T)^T\mathbf{X} + \mathbf{X}(\mathbf{A} - \mathbf{B}\mathbf{R}^{-1}\mathbf{S}^T) - \mathbf{X}\mathbf{B}\mathbf{R}^{-1}\mathbf{B}^T\mathbf{X} + \mathbf{Q} - \mathbf{S}\mathbf{R}^{-1}\mathbf{S}^T = \mathbf{0}. \tag{63}$$

The optimal performance, J^*, can be found from the relation

$$J^* = \mathrm{tr}(\mathbf{Q}\mathbf{P} + \mathbf{K}^T\mathbf{R}\mathbf{K}\mathbf{P}) \tag{64}$$

where $\mathbf{P}$ is the positive semidefinite solution to the Lyapunov equation

$$(\mathbf{A} - \mathbf{B}\mathbf{R}^{-1}\mathbf{S}^T - \mathbf{B}\mathbf{K})\mathbf{P} + \mathbf{P}(\mathbf{A} - \mathbf{B}\mathbf{R}^{-1}\mathbf{S}^T - \mathbf{B}\mathbf{K})^T + \mathbf{G}^T\mathbf{G} = \mathbf{0}. \tag{65}$$

This suspension is optimized three times, using a sequential, simultaneous, and CPF formulation, and the results are then compared.

4.2.1. Sequential optimization of automotive suspension

In the sequential optimization problem, the passive suspension is first optimized for ride quality, with the artifact design variables chosen as k_s and c_s. For this problem, J_q is calculated with the controller gains, $\mathbf{K}$, set to zero, and therefore it is a function only of the artifact design variables. The optimization problem is constrained by upper and lower bounds on both k_s and c_s. This also ensures that all of the eigenvalues of $\mathbf{A}$ must be stable, i.e., they must all lie in the left half of the complex plane. After this optimization is performed, the optimal gains for the active suspension design are found for different values of r_3, producing a set of optimal controllers which show a trade-off between ride quality and control effort. This formulation is expressed by the following equations:

$$\min_{k_s, c_s} \quad J_{q_{pas}}(k_s, c_s) \tag{66}$$

$$\text{subject to} \quad 1.6\ \text{kN/m} \leqslant k_s \leqslant 160\ \text{kN/m} \tag{67}$$

$$0.16\ \text{kN s/m} \leqslant c_s \leqslant 16\ \text{kN s/m} \tag{68}$$

followed by

$$\min_{\mathbf{K}} J_q(k_s^*, c_s^*, \mathbf{K}) + r_3 J_u(k_s^*, c_s^*, \mathbf{K}) \tag{69}$$

where $k_s^*, c_s^* = \mathrm{argmin} J_{q_{pas}}(k_s, c_s), J_{q_{pas}} = \mathrm{tr}(\mathbf{Q}\mathbf{P}_{\mathbf{pas}})$, and $\mathbf{P}_{\mathbf{pas}}$ solves the Lyapunov equation

$$\mathbf{A}\mathbf{P}_{\mathbf{pas}} + \mathbf{P}_{\mathbf{pas}}\mathbf{A}^T + \mathbf{G}^T\mathbf{G} = \mathbf{0}. \tag{70}$$

4.2.2. Simultaneous optimization of automotive suspension

In the simultaneous optimization, the total system objective, J, will be optimized for different values of r_3. In this case, the design variables for the optimization are the artifact design variables, k_s and c_s, and the controller gains, $\mathbf{K}$. The upper and lower bounds on the spring constant and damping are also included in this formulation, and the controlled system is required to be stable. In this case, the objective function is dependent on all variables, and the optimization problem is expressed as:

$$\min_{k_s, c_s, \mathbf{K}} \quad J_q(k_s, c_s, \mathbf{K}) + r_3 J_u(k_s, c_s, \mathbf{K}) \tag{71}$$

$$\text{subject to} \quad 1.6\ \text{kN/m} \leqslant k_s \leqslant 160\ \text{kN/m} \tag{72}$$

$$0.16\ \text{kN s/m} \leqslant c_s \leqslant 16\ \text{kN s/m} \tag{73}$$

$$\mathbf{g}(k_s, c_s, \mathbf{K}) = \mathrm{real}(\mathrm{eig}(\mathbf{A} - \mathbf{B}\mathbf{K})) \leqslant \mathbf{0} \tag{74}$$

As in the sequential formulation, a set of designs is obtained which show a trade-off between the ride quality and control effort.

4.2.3. Optimization of automotive suspension using a CPF

It initially appears that this problem may not be amenable to the use of a CPF, since both the ride quality, J_q, and the control effort, J_u, depend on the artifact and controller design variables. Because of this dependence, this system presents bi-directional coupling, in contrast to the positioning gantry, while the development of the CPF method was based on the assumption of uni-directional coupling. However, the ride quality can be separated into two components, with one of those components dependent only on the artifact design variables.

Assume that the matrix $\mathbf{P}$ is expressed as the sum of two matrices, $\mathbf{P}_{\mathbf{pas}}$ and $\mathbf{P}_{\mathbf{act}}$, where $\mathbf{P}_{\mathbf{pas}}$ is defined as in Eq. (70). Then, the active component of $\mathbf{P}$ satisfies the equation

$$(\mathbf{A} - \mathbf{B}\mathbf{R}^{-1}\mathbf{S}^T - \mathbf{B}\mathbf{K})\mathbf{P}_{\mathbf{act}} + \mathbf{P}_{\mathbf{act}}(\mathbf{A} - \mathbf{B}\mathbf{R}^{-1}\mathbf{S}^T - \mathbf{B}\mathbf{K})^T - (\mathbf{B}\mathbf{K}\mathbf{P}_{\mathbf{pas}} + \mathbf{P}_{\mathbf{pas}}\mathbf{K}^T\mathbf{B}^T) = \mathbf{0} \tag{75}$$

This allows the ride quality to be expressed as two separate components, one purely passive and one combining active and passive characteristics, where

$$J_q = J_{q_{act}} + J_{q_{pas}} = \mathrm{tr}(\mathbf{Q}\mathbf{P}_{\mathbf{act}}) + \mathrm{tr}(\mathbf{Q}\mathbf{P}_{\mathbf{pas}}) \tag{76}$$

and the objective function, J, can be decomposed into two functions, $f_a(\mathbf{d_a})$ and $f_c(\mathbf{d_a}, \mathbf{d_c})$, as follows:

$$f_a(\mathbf{d_a}) = J_{q_{pas}}(k_s, c_s) \tag{77}$$

$$f_c(\mathbf{d_a}, \mathbf{d_c}) = J_{q_{act}}(k_s, c_s, \mathbf{K}) + r_3 J_u(k_s, c_s, \mathbf{K}) \tag{78}$$

By decomposing the problem in this way, it can be shown that a CPF may be effective, although the optimization does not exactly match any of the formulations where a perfect CPF is known to exist. Since the problem does not match any of the cases that led to a perfect CPF, it cannot be assumed that such a perfect CPF necessarily exists. Because one component of f_c is the control effort, however, it can be postulated that a CPF based on the controllability Grammian matrix will produce results that are close to optimal.

The optimization problem using a CPF is formulated as follows:

$$\min_{k_s, c_s} \quad J_{q_{pas}}(k_s, c_s) + r_4\chi(k_s, c_s) \tag{79}$$

$$\text{subject to} \quad 1.6\ \text{kN/m} \leqslant k_s \leqslant 160\ \text{kN/m} \tag{80}$$

$$0.16\ \text{kN s/m} \leqslant c_s \leqslant 16\ \text{kN s/m} \tag{81}$$

followed by

$$\min_{\mathbf{K}} \quad J_q(k_s^*, c_s^*, \mathbf{K}) + r_3 J_u(k_s^*, c_s^*, \mathbf{K}) \tag{82}$$

$$\text{subject to} \quad \mathbf{g}(k_s, c_s, \mathbf{K}) = \mathrm{real}(\mathrm{eig}(\mathbf{A} - \mathbf{B}\mathbf{K})) \leqslant \mathbf{0} \tag{83}$$

where the CPF is chosen as

$$\chi(k_s, c_s) = \frac{1}{\det\left(\mathbf{W}_\mathbf{c}^{\infty}\right)} \tag{84}$$

This CPF is chosen in order to ensure that the suspension is controllable. The CPF will be minimized when the determinant of the controllability Grammian is at its maximum, which indicates that the system requires less control effort in order to meet the control objectives. This optimization can be performed for various different combinations of r_4 and r_3; here, we perform the optimization for two fixed values of r_4. For each value of r_4, we obtain a passive design, and then vary r_3 to explore the active performance of that passive design.

4.2.4. Comparison of optimal designs

Results of these three optimization problems are shown in Fig. 6 for the cases where $r_4 = 2.5e{-}30$ and $r_4 = 3.5e{-}30$, where these values of r_4 were empirically chosen to represent the cases of more expensive and less expensive control. The values of the variables and objectives are also given in Table 2. In the case of expensive control, i.e., $r_3 \to \infty$, the results of sequential and simultaneous optimizations converge, as do the results for both of the optimizations using a CPF. The optimal performance of the suspension designed using a CPF is an improvement over the sequential solution, though it does not match the simultaneous solution for finite values of r_3. For these high values of r_3, the better of the two CPF solutions is that with the higher value, i.e., $r_4 = 3.5e{-}30$.

When the control cost is lower, then the sequential and simultaneous designs show a greater difference. The suspension designed sequentially is unable to match the results of the simultaneous optimization. Again, the solution found using a CPF represents an improvement over the sequential solution; it is extremely close to the optimal results found from the simultaneous formulation.

As the value of r_3 is decreased, the relative quality of the two CPF solutions reverses. As control becomes less expensive, the solution found with a lower weight on the CPF, i.e., $r_4 = 2.5e{-}30$, shows better results. In fact, as control becomes even less expensive, the solution found with the greater value of r_4 is farther from the optimal results than the sequential solution.

The choice of r_4, then, should be made based on the designer's expectations about the cost of control; if control is expected to be 'cheap', i.e., $r_3 \to 0$, then r_4 should be relatively small. If control is expected to be expensive, then r_4 should be larger.

Again, the advantage of solving the optimization problem using a CPF is that it allows the design and control optimizations to be carried out separately. The designer of the automotive suspension system then would not need to also design the control system, and in fact would not even need to know what type of control would be designed; he or she would only need to know whether control was expected to be expensive or cheap in order to choose an appropriate weight for the CPF (see Table 2).

Consider a weight of $r_3 = 2.66e{-}7$ for all of the optimization formulations. For this weight, each of the methods of solution produces the same result for the optimal value of c_s, which is the upper bound on the variable. In contrast, each method yields a different result for the stiffness of the spring. The sequentially optimized design has a relatively stiff spring, with a softer spring found in the simultaneous solution. The spring stiffness for both of the CPF problems is less than that of the simultaneous formulation, which increases the controllability and thus decreases the

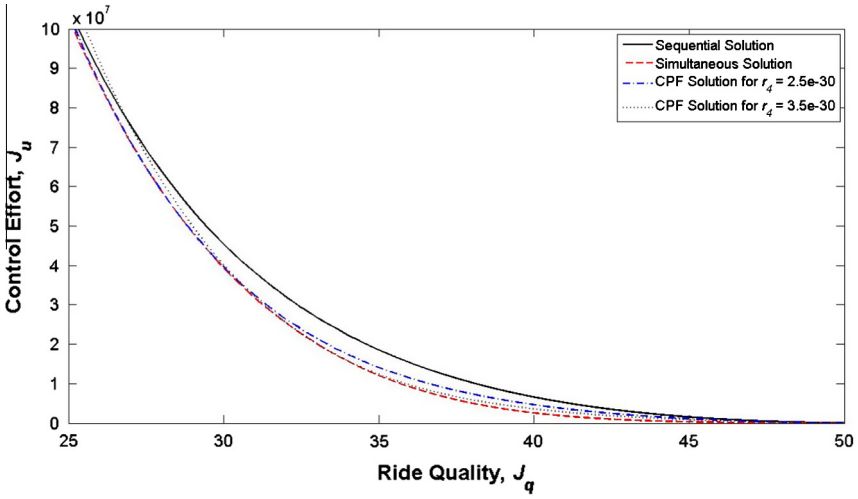

Fig. 6. Optimal performance of active/passive suspension.

Table 2
Comparison of optimal designs for $r_3 = 2.66e{-}7$.

	Sequential	Simultaneous	CPF with $r_4 = 2.5e{-}30$	CPF with $r_4 = 3.5e{-}30$
k_s (kN/m)	36.0	9.26	18.1	10.9
c_s (kN s/m)	16.0	16.0	16.0	16.0
K	$\begin{bmatrix} 989.1 \\ 155.7 \\ -2087 \\ -1763 \end{bmatrix}^T$	$\begin{bmatrix} -1394 \\ 167.5 \\ -6281 \\ -3648 \end{bmatrix}^T$	$\begin{bmatrix} 78.01 \\ 163.0 \\ -3879 \\ -2660 \end{bmatrix}^T$	$\begin{bmatrix} -992.2 \\ 166.6 \\ -5655 \\ -3408 \end{bmatrix}^T$
J_q	34.52	34.28	33.84	34.09
J_u	2.030e7	1.460e7	1.803e7	1.541e7

control effort required. All four sets of results have similar values for the ride quality, with the highest and lowest ride quality differing by less than 2%; however, there are significant differences of up to 39% in the control effort required to achieve this ride quality. The greatest amount of control effort is required by the sequentially optimized design, and the least control effort for the simultaneously optimized design. The two designs found through optimization using a CPF are both better than the sequentially optimized design; for the CPF design with $r_4 = 2.5e{-}30$, the control effort is 23% greater than that for the simultaneous design, representing a substantial improvement over the sequential design. By increasing the weight on the CPF to $r_4 = 3.5e{-}30$, the control effort required can be further reduced, to only 5% greater than that required by the simultaneous design. This demonstrates that a solution method using a CPF can provide improved results over a simple sequential solution, while retaining the decomposition advantages of the sequential solution method.

5. Concluding remarks

In this paper, a new method of solution for co-design problems, based upon a sequential optimization using a Control Proxy Function (CPF) is presented. The intent of the CPF method is to provide solutions that are identical with, or close to, the Pareto optimal solutions to the co-design problem, while allowing the problem to be decomposed into an artifact design problem and a control design problem. It may be desirable in some cases to formulate co-design problems without performing this decomposition, particularly when a single metric can adequately capture the system's desired performance. However, decomposing the system into the two domains of artifact and controller allows the co-design problem to be more easily formulated and solved by experts in each of the functional areas of artifact design and control design, and is particularly useful when there is some degree of separation naturally present in the system.

The key to the effectiveness of this method is the choice of an appropriate CPF, and we have proposed appropriate CPFs for specific problem formulations. These CPFs are based on the system's natural frequency and on the controllability Grammian matrix. In the case of both CPFs, we have assumed that the system of interest is linear and time-invariant. For a CPF based on natural frequency, the system was also assumed to be second-order, though the CPF based on the controllability Grammian applies to systems of arbitrarily high order. One of these CPFs, based on the natural frequency, was used in the optimization of a simple positioning gantry and its controller, and was shown to provide optimal solutions. Similarly, a CPF based on the controllability Grammian matrix was used in the optimization of an automotive suspension with both passive and active components. While these systems are relatively simple, they show that the method can be quite effective. In larger-scale systems, the use of a CPF could be incorporated into a large all-in-one optimization problem, or multiple CPFs could be used for individual components within an optimization structure incorporating decomposition and coordination. Use of the method on such larger scale systems should be a subject of future work, as should the integration of the method into engineering practice in industry. Such use within industry will require several advances. These include the extension of the method to cover a wider range of problems and the formulation of a clear, easily followed procedure by which a designer may check to ensure that the method is appropriate and select the proper CPF for the design problem under consideration. Such a procedure could take the form proposed in [8], in which a series of system and problem characteristics were checked to ensure that the method was appropriate for the particular problem.

These CPFs are not exhaustive; it is possible to formulate and evaluate additional CPFs, based on open-loop eigenvalues, the controllability Grammian, and possibly other system metrics, and the development of such CPFs should be the subject of future work. These CPFs could be used to produce optimal solutions for a variety of problems not considered here, such as Linear Quadratic Gaussian (LQG) control, vehicle steering applications, trajectory control, sensor placement, and power management. In some cases, such as the automotive suspension demonstrated here, it may not be possible to develop a simple CPF that provides optimal results. However, one can conjecture that a CPF based on the controllability and observability Grammians will produce results that are near-optimal for a variety of problems, since they provide measures of how easily a system is controlled and how easily the states are estimated. This conjecture should also be investigated in future work, and it should be determined how effective a CPF based on the controllability and observability Grammians will be for various types of co-design problems. Future work should also investigate ways in which this technique could be applied to problems with bi-directional coupling, as well as non-linear systems with both uni-directional and bi-directional coupling, and the technique should be applied to larger scale problems of interest.

Acknowledgements

This work was partially supported by NSF Grant # 0625060 and by the Automotive Research Center (ARC), a US Army Center of Excellence in Modeling and Simulation of Ground Vehicles, headquartered at the University of Michigan. This support is gratefully acknowledged.

References

[1] Haftka R, Martinovic Z, Hallauer Jr W, Schamel G. An analytical and experimental study of a control system's sensitivity to structural modifications.. AIAA J 1986;25:310–5.
[2] Bloebaum C. Coupling strength-based system reduction for complex engineering design. Struct Optim 1995;10:113–21.
[3] Fathy H, Papalambros PY, Ulsoy AG. On combined plant and control optimization. In: 8th Cairo University international conference on mechanical design and production. Cairo, Egypt: Cairo University; 2004.
[4] Alyaqout SF, Papalambros PY, Ulsoy AG. Quantification and use of system coupling in decomposed design optimization problems. In: Proceedings of the ASME IMECE 2005. ASME, Orlando, FL; 2005. p. 95–103, paper number IMECE2005-81364.
[5] Alyaqout SF, Papalambros PY, Ulsoy AG. Coupling in design and robust control optimization. In: Proceedings of the European control conference. Kos, Greece; 2007.
[6] Alyaqout SF, Peters DL, Papalambros PY, Ulsoy AG. Generalized coupling management in complex engineering systems optimization. ASME J Mech Des 2011;133(9).
[7] Peters DL, Papalambros PY, Ulsoy. On measures of coupling between the artifact and controller optimal design problems. In: Proceedings of the ASME design engineering technical conference & computers in engineering conference. ASME, San Diego, CA; 2009, paper number DETC 2009-86868.
[8] Peters DL. Coupling and controllability in optimal design and control, PhD thesis. University of Michigan, Ann Arbor, MI; April 2010.
[9] Peters DL, Papalambros PY, Ulsoy AG. Control proxy functions for sequential design and control optimization. ASME J Mech Des 2011;133(9).
[10] Fathy HK, Reyer JA, Papalambros PY, Ulsoy AG. On the coupling between the plant and controller optimization problems. In: Proceedings of the American control conference. Arlington, VA: IEEE; 2001. p. 1864–9.
[11] Rao S, Pan T. Modeling, control, and design of flexible structures: a survey. Appl Mech Rev 1990;43:99–117.
[12] Carley L, Ganger G, Guillou D, Nagle D. System design considerations for MEMS-actuated magnetic-probe-based mass storage. IEEE Trans Magn 2001;37:657–62.
[13] Oldham K, Huang X, Chahwan A, Horowitz R. Design, fabrication and control of a high-aspect ratio microactuator for vibration suppression in a hard disk drive. In: Proceedings of the IFAC world congress. Prague; 2005.
[14] Alyaqout SF, Papalambros PY, Ulsoy AG. Combined design and robust control of a vehicle passive/active suspension. In: Proceedings of the European control conference. Kos, Greece; 2007.
[15] Alyaqout SF, Papalambros PY, Ulsoy AG. Combined design and robust control of a vehicle passive/active suspension. Int J Veh Des 2012;59(4):315–30.

[16] Alyaqout SF, Papalambros PY, Ulsoy AG. Combined robust design and robust control of an electric DC motor. In: ASME international mechanical engineering congress and exposition. ASME, Chicago, IL; 2006.
[17] Alyaqout SF, Papalambros PY, Ulsoy AG. Combined robust design and robust control of an electric DC motor. IEEE/ASME Trans Mech 2011;16(3):574–82.
[18] Ravichandran T, Wang D, Heppler G. Simultaneous plant-controller design optimization of a two-link planar manipulator. Mechatronics 2006;16:233–42.
[19] Zhu Y, Qiu J, Tani J. Simultaneous optimization of a two-link flexible robot arm. J Robotic Syst 2001;18(1):29–38.
[20] Akdoğan E, Adli MA. The design and control of a therapeutic exercise robot for lower limb rehabilitation: Physiotherabot. Mechatronics 2011;21:509–22.
[21] Rieber JM, Taylor DG. Integrated control system and mechanical design of a compliant two-axes mechanism. Mechatronics 2004;14:1069–87.
[22] Ouyang P, Li Q, Zhang WJ, Guo L. Design, modeling and control of a hybrid machine system. Mechatronics 2004;14:1197–217.
[23] Rao JS, Tiwari R. Design optimization of double-acting hybrid magnetic thrust bearings with control integration using multi-objective evolutionary algorithm. Mechatronics 2009;19:945–64.
[24] Rodriguez-Fortun JM, Orus J, Alfonso J, Sierra JR, Buil F, Rotella F, et al. Model-based mechanical and control design of a three-axis platform. Mechatronics 2012;22:958–69.
[25] Ouyang P, Zhang W, Wu F. Nonlinear PD control for trajectory tracking with consideration of the design for control methodology. In: Proceedings of the IEEE international conference on robotics & automation. Washington, DC: IEEE; 2002. p. 4126–31.
[26] Park J, Asada H. Integrated structure/control design of a two-link nonrigid robot arm for high speed positioning. In: Proceedings of the IEEE international conference on robotics & automation. Nice, France: IEEE; 1992.
[27] Reyer J. Combined embodiment design and control optimization: effects of cross-disciplinary coupling, PhD thesis. University of Michigan, Ann Arbor, MI; April 2000.
[28] Fathy H. Combined plant and control optimization: theory, strategies and applications, PhD thesis. University of Michigan, Ann Arbor, MI; April 2003.
[29] Ross IM, Fahroo F. Legendre pseudospectral approximations of optimal control problems. In: Lecture notes in control and information sciences, vol. 295. New York, NY; 2003. p. 327–42.
[30] Peters DL, Papalambros PY, Ulsoy AG. Sequential co-design of an artifact and its controller via control proxy functions. In: 5th IFAC symposium on mechatronic systems, cambridge. MA; 2010.
[31] Peters DL, Kurabayashi K, Papalambros PY, Ulsoy AG. Co-design of a MEMS actuator and its controller using frequency constraints. In: Proceedings of the ASME dynamic systems and control conferences. ASME, Ann Arbor, MI; 2008. paper number DSCC 2008-2212.
[32] Hale A, Lisowski R, Dahl W. Optimal simultaneous structural and control design of maneuvering flexible spacecraft. J Guid Control Dynam 1985;8:86–93.
[33] Khot N, Abhyankar N. Integrated optimum structural and control design. In: Kamat MP. editor. Structural optimization: status and promise. Washington, D.C.; 1993.
[34] Muller PC, Weber HI. Analysis and optimization of certain qualities of controllability and observability for linear dynamical systems. Automatica 1972;8:237–46.
[35] Roh H, Park Y. Actuator and exciter placement for flexible structures. J Guid Control Dynam 1997;20(5):850–6.
[36] Lim K, Gawronski W. Modal Grammian approach to actuator and sensor placement for flexible structures. AIAA J 1993;31:674–84.
[37] Peters DL, Papalambros PY, Ulsoy AG. Relationship between coupling and the controllability Grammian in co-design problems. In: Proceedings of the American control conference. Baltimore, MD: IEEE; 2010.
[38] Pomrehn L, Papalambros P. Global and discrete constraint activity. ASME J Mech Des 1994;116:745–8.
[39] Franklin G, Powell J, Emami-Naeini A. Feedback control of dynamic systems. Reading, MA: Addison-Wesley Publishing Company; 1994.
[40] Skogestad S, Postlethwaite I. Multivariable feedback control: analysis and design. West Sussex, UK: John Wiley and Sons, Ltd.; 2005.
[41] Ulsoy AG, Peng H, Çakmakci M. Automotive control systems. Cambridge, UK: Cambridge University Press; 2012.
[42] Bryson A, Ho Y. Applied optimal control. New York, NY: Hemisphere Publishing Corporation; 1975.
[43] Anderson B, Moore J. Optimal control: linear quadratic methods. Mineola, NY: Dover Publications Inc.; 1990.